JOURNAL OF VIROLOGY, Dec. 2002, p. 12691–12702 Vol. 76, No. 24
0022-538X/02/$04.00+0 DOI: 10.1128/JVI.76.24.12691–12702.2002

Effects of Membrane Potential and Sphingolipid Structures on Fusion of Semliki Forest Virus

Andrey V. Samsonov,[1]† Prodyot K. Chatterjee,[2] Vladimir I. Razinkov,[1]‡ Christina H. Eng,[2]§ Margaret Kielian,[2] and Fredric S. Cohen[1]*

Rush Medical College, Department of Molecular Biophysics and Physiology, Chicago, Illinois 60612,[1] *and Albert Einstein College of Medicine, Department of Cell Biology, Bronx, New York 10461*[2]

Received 1 April 2002/Accepted 30 August 2002

Cells expressing the E1 and E2 envelope proteins of Semliki Forest virus (SFV) were fused to voltage-clamped planar lipid bilayer membranes at low pH. Formation and evolution of fusion pores were electrically monitored by capacitance measurements, and membrane continuity was tracked by video fluorescence microscopy by including rhodamine-phosphatidylethanolamine in the bilayer. Fusion occurred without leakage for a negative potential applied to the *trans* side of the planar membrane. When a positive potential was applied, leakage was severe, obscuring the observation of any fusion. E1-mediated cell-cell fusion occurred without leakage for negative intracellular potentials but with substantial leakage for zero membrane potential. Thus, negative membrane potentials are generally required for nonleaky fusion. With planar bilayers as the target, the first fusion pore that formed almost always enlarged; pore flickering was a rare event. Similar to other target membranes, fusion required cholesterol and sphingolipids in the planar membrane. Sphingosine did not support fusion, but both ceramide, with even a minimal acyl chain (C_2-ceramide), and lysosphingomyelin (lyso-SM) promoted fusion with the same kinetics. Thus, unrelated modifications to different parts of sphingosine yielded sphingolipids that supported fusion to the same degree. Fusion studies of pyrene-labeled SFV with cholesterol-containing liposomes showed that C_2-ceramide supported fusion while lyso-SM did not, apparently due to its positive curvature effects. A model is proposed in which the hydroxyls of C-1 and C-3 as well as N of C-2 of the sphingosine backbone must orient so as to form multiple hydrogen bonds to amino acids of SFV E1 for fusion to proceed.

An enveloped virus deposits its genome into a cell by passing the genome through a fusion pore, thus initiating infection. Depending on the viral family, the pores form either directly with the plasma membrane or, after receptor-mediated endocytosis, with the endosomal membrane. For viruses that fuse with the plasma membrane, binding to receptors and/or coreceptors of the target cell induces the conformational changes in the viral proteins that lead to fusion. In contrast, most viruses that fuse within an endosome use the low endosomal pH to induce all the required conformational changes (21). For other viruses, it appears that the fusion proteins undergo initial conformational changes at the plasma membrane as a result of receptor binding and, after endocytosis, undergo additional changes induced by low pH within the endosomes (43).

Members of the alphavirus family, such as Semliki Forest virus (SFV), fuse at low pH (61). These viruses bind to protein receptors on the plasma membrane (12, 19, 36), but it appears that fusion does not require receptor binding, at least in vitro. The conformational changes that lead to fusion occur within the low-pH environment of the endosome. For SFV, the presence of cholesterol and sphingolipids in the endosomal membrane promotes the low-pH-dependent conformational changes in the fusion protein that induce membrane fusion (4, 8, 27). Cholesterol and sphingolipids are also required for fusion of Sindbis virus, another alphavirus (57). The presence of cholesterol facilitates fusion for some other viruses as well: for example, the flavivirus tick-borne encephalitis virus (11). Interactions between membrane proteins and cholesterol and sphingolipids are thought to be important not only for alphavirus fusion but for a wide range of cellular processes such as signal transduction and the generation of cell surface polarity (22, 29, 54, 55). Studying the fusion protein of SFV thus provides a means to explore not only membrane fusion but also how interactions of lipids can affect protein function in a well-defined biological setting.

The membrane protein of SFV, directly responsible for inducing fusion, is a trimer comprised of heterotrimers of E1/E2/E3 subunits. E1 and E2 are type I transmembrane glycoproteins; E3 is a peripheral glycoprotein and is not required for fusion to occur (45, 59). E2 is the dominant subunit responsible for binding to cells, while E1 mediates membrane fusion (28). At low pH, a series of conformational changes occur that result in the separation of E1 from E2, the insertion of the fusion peptide of E1 into the target membrane, and the association of three E1 monomers to form a highly stable E1 homotrimer. The presence of cholesterol and sphingolipids promotes both the insertion of the fusion peptide and the conversion of the E1 protein to the fusion-active conformation (4, 27, 44). Sphingosine is the central structure of all sphingolipids, but sphingosine itself does not support fusion; at least one additional

* Corresponding author. Mailing address: Department of Molecular Biophysics and Physiology, Rush Medical College, 1653 W. Congress Pkwy., Chicago, IL 60612-3824. Phone: (312) 942-6753. Fax: (312) 942-8711. E-mail: fcohen@rush.edu.

† Present address: University of Illinois Medical School, Department of Physiology and Biophysics, Chicago, IL 60612.

‡ Present address: Wyeth-Ayerst Research, Pearl River, NY 10965.

§ Present address: Integrated Program in Cellular, Molecular and Biophysical Studies, College of Physicians and Surgeons, Columbia University, New York, NY 10032.

structure must be attached to it. Ceramide, sphingosine with one added acyl chain, is the minimal sphingolipid structure that permits fusion (44). The features of the sphingosine backbone required for fusion have also been identified. The 3-hydroxy group and the 4,5-*trans* carbon-carbon double bond of sphingosine are essential for a sphingolipid to support fusion (10). These lipid requirements were identified from population measurements of extents and kinetics of the fusion of virus to liposomes. However, since the best way to obtain kinetics is at the level of single events and since such investigations had never before been conducted, we undertook this study.

We fused cells expressing the membrane protein of SFV (E1/E2/E3) to planar lipid bilayer membranes because the lipid composition and the membrane potential of the planar membrane are both conveniently controlled and because individual fusion events can be measured by both time-resolved admittance (capacitance) measurements and video fluorescence microscopy (40, 51). We show that fusion without leakage occurs quickly when a *trans*-negative potential is present across the planar membrane; fusion does not occur over comparable times for a *trans*-positive potential, but substantial leakage does occur. These findings suggest that, for SFV E1, the endosomal membrane potential may be an important biological regulator for controlling proper insertion of the fusion protein into the membrane. If this is true, it would demonstrate an unusual mechanism for insertion in fusion. We also further explored the structural requirements for a sphingolipid to support fusion, leading us to the hypothesis that sphingolipids can support fusion only if the structure of the hydroxyl and the amine (or the amide) groups that can hydrogen bond to E1 are rotationally constrained.

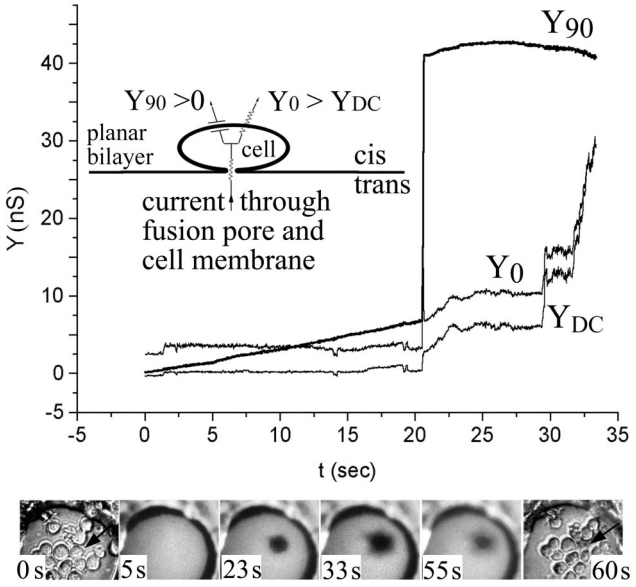

FIG. 1. Cell fusion is triggered at low pH under conditions of *trans*-negative potential. HEK 293T cells expressing E1/E2 were fused to a planar membrane composed of DOPC–DOPE–cholesterol–SM–rho-PE (in moles percent, 41/20/25/5/9) with a −40 mV potential applied to the *trans* solution. Fusion was triggered by adjusting the pH to 5.6 ($t = 0$). Electrical traces (top panel): upon fusion, the pore quickly enlarged. This was observed as both a fast, step-like increase in Y_{90} and a transient increase in Y_0 that returned to the sloping baseline. The increase in Y_{DC} shows that the membrane became leaky. In this experiment, fusion occurred somewhat more slowly after acidification and leakage was somewhat less severe than was typical. Images (lower panel): the first and last images show the cells in bright-field microscopy, before and after fusion. The four middle panels show fluorescence images at the indicated times. Soon after a pore enlarged as determined electrically, the rho-PE-labeled planar membrane became dark at the site of the fused cell (marked by an arrow in the two bright-field images). This is the pattern of fluorescence expected of full pore enlargement. The cell lost bright-field contrast after fusion.

MATERIALS AND METHODS

Materials. Squalene was obtained from ICN Biomedicals, Inc. (Aurora, Ohio). Hexane, hemisynthetic *N*-stearoyl-sphingomyelin (SM) and *N*-oleoyl-SM were purchased from Sigma Chemical Co. (St. Louis, Mo.). All fluorescent probes were obtained from Molecular Probes (Eugene, Oreg.). Sphingosine-1-phosphate was purchased from Matreya, Inc. (Pleasant Gap, Pa.). Cholesterol, phospholipids, rhodamine (rho)-dioleoylphosphatidylethanolamine (DOPE), egg SM, and all other sphingolipids were purchased from Avanti Polar Lipids (Alabaster, Ala.).

Planar membrane formation. Solvent-free horizontal bilayers were formed from a solution of dioleoylphosphatidylcholine (DOPC)-DOPE maintained at a 2:1 ratio and 20 to 25 mol% cholesterol, 5 to 10 mol% sphingolipid, and 9 mol% rho-DOPE (the "base" composition) in squalene. Any impurities in the squalene were removed by passing it through a column of activated aluminum oxide. Planar membranes were formed by a brush technique in a 150- to 200-μm-diameter hole in a Teflon film and were bathed by symmetrical solutions of 140 mM NaCl, 2.5 mM KCl, 5 mM $MgCl_2$, 2 mM $CaCl_2$, and 1 mM HEPES, pH 7.0. The temperature of the solution was maintained with a temperature controller (20/20 Technology Inc., Wilmington, N.C.). We used 15°C for fusion experiments, as this temperature yielded fast and efficient fusion and as the leaks that are associated with fusion were smaller than those that occur at higher temperatures. In a few experiments at 10°C, fusion occurred efficiently, although somewhat more slowly than at 15°C, but the leakage was not obviously lessened.

Transient expression of SFV envelope proteins in HEK 293T cells. The structural proteins of wild type SFV and the srf-3 mutant were expressed in HEK 293T cells by using pCB3-wt and pCB3-srf-3 plasmid constructs, respectively, and were transfected by a standard calcium phosphate precipitation method (34). In brief, an *Eco*RI-*Hin*dIII fragment encoding the wild-type SFV structural proteins capsid, p62, 6K, and E1 was ligated with the *Eco*RI-*Hin*dIII fragment of the pCB3 vector containing the cytomegalovirus promoter and simian virus 40 origin to give pCB3-wt. An *Eco*RV-*Hin*dIII fragment from the srf-3 infectious clone (60) was exchanged with this fragment in the pCB3-wt to give pCB3-srf-3 containing the srf-3 mutation (E1 P226S).

Fusion pore measurements. HEK 293T cells were used for fusion experiments 48 h after transfection with the pCB3-wt or pCB3-srf-3 plasmid. At that time, the cells were removed from culture dishes with divalent cation-free phosphate-buffered saline containing EDTA and EGTA and were then concentrated (in phosphate-buffered saline to $\sim 10^7$ cells per ml). When a few microliters of this cell suspension was layered above a horizontal voltage-clamped planar membrane, about 5 to 10 cells settled on the membrane within 1 min. After the cells were allowed to adhere for an additional 1 to 2 min, fusion was triggered by lowering the pH of the top, cell-containing (*cis*) solution to 5.6 by injecting a small amount (e.g., 25 μl) of an isotonic *N*-methyl-D-glucamine–L-glutamic acid solution from a pipette placed directly over the bilayer. This pH 5.6 solution was heavy and readily displaced the preexisting solution (within 2 s of its addition, as determined from a small increase in Y_0, where Y denotes admittance). Fusion pore formation was monitored by time-resolved electrical admittance measurements as described earlier (39). Briefly, the increment of cell capacitance due to pore formation between cell and planar bilayer was measured by applying a 20-mV peak-to-peak sine wave voltage of 1-kHz frequency. The in-phase (Y_0), out-of-phase (Y_{90}), and direct current (Y_{DC}) components of admittance were calculated in real time with a software-based phase detector (49), and pore conductance was obtained. When fusion occurs, a sine wave current flows between the *trans* and *cis* solutions via the fusion pore and cell capacitance (which, electrically, are in series). Fusion thereby results in an increase in both Y_0 and Y_{90} (Fig. 1,inset). If the cell membrane is leaky, Y_{DC} also increases concomitantly with fusion and $Y_0 > Y_{DC}$. Any leaks that occur in the planar bilayer (whether or not fusion occurs) result in a flow of current directly between the *cis* and *trans* solutions, which also causes an increase in Y_{DC}, but in this case $Y_0 = Y_{DC}$.

The sine wave voltage was superimposed on a DC holding potential. In addition to the clamped holding potential, there could be a diffusion potential across the membrane when a pH gradient was established. It is difficult to unambiguously determine reversal potentials for high-resistance (e.g., >10 GΩ) membranes. But for pH 7.0 on the *trans* side, pH 5.6 on the *cis* side, as in fusion experiments, the reversal potential was small, at most 10 to 20 mV *trans* positive (data not shown). We therefore ignored the diffusion potential and considered the membrane potential to be the applied potential even when a pH gradient across the bilayer was maintained. We used an applied *trans*-negative 40 mV potential, unless indicated otherwise. The fluorescent lipid rho-phosphatidylethanolamine (PE) was included in the planar membrane at a self-quenching concentration (9 mol%) so that spread of dye upon hemifusion or fusion could be monitored by video microscopy. For all lipid mixtures (including those that contained C_2-ceramide and ceramides with longer chains), the conductance of the bilayer was small (<100 pS) and was stable in the absence of cells. This contrasts to the finding that the addition of ceramides to the aqueous phase leads to the formation of large channels in lipid bilayer membranes (56).

Due to substantial variation in SFV protein expression levels and the condition of cell cultures, at least two different membrane compositions were prepared during each day of experiments and were compared to determine the efficacy of a sphingolipid to support fusion. This allowed results to be compared so that conclusions were not dependent on any characteristics other than the type of sphingolipid within the membrane. The base composition provided a consistent point of reference. Kinetics of fusion were characterized on the level of single events from waiting-time distributions. These yielded the probability that a fusion event would occur at a time later than time t (see Fig. 6). For example, pores had not yet formed at the moment of acidification, i.e., $t = 0$ (i.e., all pores would form at a later time). Hence, this probability at $t = 0$ was 1, from which the waiting- time distributions monotonically decayed. This probability was given by $N(t)/N(0)$, where $N(0)$ was the total number of pores measured for all experiments and where $N(t)$ was the number of pores that formed at times that were $> t$. The waiting time from acidification until the first fusion event was obtained for each experiment, and all waiting times were gathered to generate the distribution of waiting times: $[N(t)/N(0)]$.

Measuring syncytium formation. 293T cells were grown to 40 to 50% confluency on circular 12-mm-diameter coverslips that were placed in a 60-mm culture dish and were then transfected. Forty-eight hours later, calcein-acetoxymethyl (AM) was loaded into the cells according to the manufacturer's specifications. The coverslips were transferred to 35-mm-diameter dishes containing either a high-Na^+-content or high-K^+-content medium (120 mM KCl, 10 mM NaCl, 5 mM $MgCl_2$, 2 mM $CaCl_2$, 5 mM HEPES, and 5 mM morpholineethanesulfonic acid, pH 7.0), always maintaining osmolarity. The pH was lowered to 5.6 by adding HCl for 3 min followed by returning to pH 7.0, all at 37°C. Because SFV-induced polykaryon formation is clearly visible by light microscopy 30 min after reduction of the pH (24, 35), the spread of calcein was measured at this time. All images of this study utilized a video camera (SIT 66; Dage, Michigan City, Ind.).

Liposome fusion assays. Pyrene-labeled SFV was prepared using wild-type SFV derived from the pSP6-SFV-4 infectious clone (33). This virus stock was propagated in BHK cells that had been prelabeled by growth for 24 h in the presence of C_{16}-pyrene (Molecular Probes). Pyrene-labeled virus was purified by banding on a sucrose gradient. Unilamellar liposomes were prepared by extrusion through two 0.2-μm-pore-size filters and were mixed with virus at the indicated liposome concentrations and lipid compositions. All phospholipids were from Avanti Polar Lipids. Each assay contained 0.6 μM virus phospholipid (calculated from a virus phospholipid-to-protein ratio of 0.45 μmol/mg of protein) in a 2-ml volume. Fusion was triggered by adjusting the liposome-virus mix to pH 5.5, and the decrease in pyrene eximer fluorescence was followed using excitation and emission wavelengths of 343 and 480 nm, respectively, in an Aminco-Bowman AB-2 fluorometer (Spectronic Unicam, Rochester, N.Y.) with a thermojacketed cuvette holder and 470-nm cutoff filter in the emission beam. The 0% fusion level was set to the initial virus excimer fluorescence, and 100% fusion was defined as the background fluorescence of target liposomes. All of these methods are described in more detail in reference 4.

RESULTS

Cells expressing SFV E1/E2 fused quickly and efficiently with planar bilayers. For each experiment, 5 to 10 cells transfected with the SFV structural proteins were settled on a horizontal planar bilayer membrane and fusion was triggered by lowering the pH to 5.6. Under optimal bilayer (e.g., SM included) composition and cell conditions (see Materials and Methods), fusion was rapid, with the majority of events occurring within 10 s of reduction of the pH of the top (*cis*) solution.

Fusion was electrically characterized as an increase in the in-phase (Y_0) and out-of-phase (Y_{90}) components of the admittance of the bilayer (Fig. 1, electrical traces). Routinely, the first pore that formed enlarged fully to conductances on the order of hundreds of nanosiemens without prior formation of flickering pores. Even for experiments in which the first enlarging pore did not form for more prolonged times (tens of seconds after reduction of the pH on SM-containing planar membranes), pronounced or obvious pore flickering was not observed. We considered whether the absence of flickering was an intrinsic property of SFV E1-induced pores or a consequence of the high cholesterol content of the bilayer membranes. In the absence of cholesterol, several flickers usually preceded full pore enlargement for pores induced by hemagglutinin (HA) of influenza virus (39). However, for bilayers containing high concentrations of cholesterol and 5 mol% SM, the first HA pore fully enlarged without prior flickering. When SM was included in high concentrations (10 mol% or above) in cholesterol-containing bilayers, flickering occurred to a greater extent than in the absence of both lipids (50). Similar experiments using cells expressing SFV E1/E2 and bilayers with 10 to 15 mol% SM plus cholesterol did not yield flickering, demonstrating that the absence of flickering pores is intrinsic to E1 of SFV.

Soon after full pore enlargement was detected electrically, a spot under a cell became dark and grew larger, with a time constant of less than 1 s (Fig. 1, images). The darkening was a visual indicator of the location of the fused cell. The maximum diameter of this dark region depended on the size of the fusing cell and ranged from about 20 to 50 μm. The darkening can be accounted for by the difference in tension between the planar membrane and cell membrane, which would cause lipid flow that displaces rho-PE of the planar membrane with nonfluorescent cell lipid (7, 40). After this darkening, the cells started to become bright, showing that the rho-PE diffusively spread into the cells (Fig. 1, images). Soon after fusion (typically after darkening), Y_{DC} and Y_0 increased in a step-like fashion and $Y_0 \approx Y_{DC}$, indicating that leaks (see Materials and Methods) had formed in the planar membrane.

Fusion requires a *trans*-negative potential. The voltage across the voltage-clamped planar membrane was routinely controlled. This allowed us to explore the effects of voltage of the target membrane on SFV fusion. Fusion always occurred ($n = 50$) when the magnitude of the potential across the voltage-clamped planar membrane was −40 mV, with the sign representing negativity on the *trans* side. The planar membrane was stable for relatively long times (for several minutes or more) after fusion occurred, despite the occurrence of leaks. In general, leaks occurred subsequent to fusion. That is, for a *trans*-negative potential, fusion was intrinsically a tight, nonleaky process. In contrast, when a +40 mV *trans*-positive membrane voltage was maintained from the start of an experiment for the same batches of cells, lowering the pH did not lead to fusion. Instead, only leaks developed (with the observed DC conductance increasing to about 10 to 30 nS) (Fig. 2), followed by the rupture of the membrane ($n = 10$). This rupture oc-

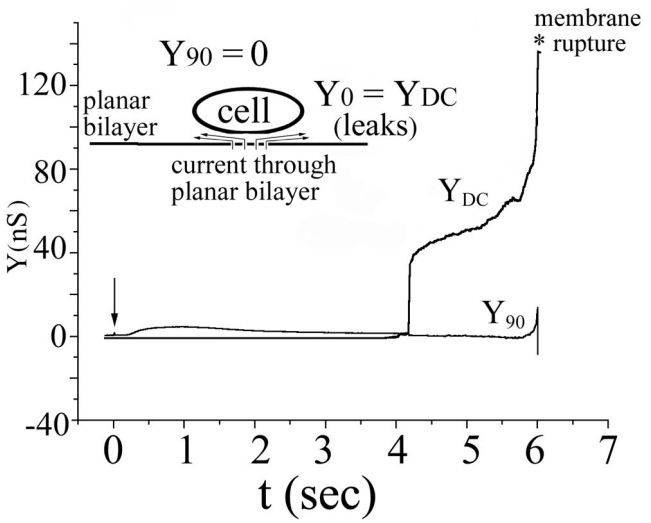

FIG. 2. Leaks, but not fusion, are triggered at low pH under conditions of *trans*-positive potentials. All conditions were the same as for Fig. 1 except that a potential of +40 mV was applied to the *trans* solution. Upon lowering of pH (arrow), Y_{DC} increased soon thereafter, indicating leakage. The absence of an increase in Y_{90} shows that fusion did not occur. The absence of fusion was confirmed by the absence of changes in the fluorescence and bright-field images (not shown). The membrane broke after the leakage became severe. For *trans*-positive potentials, fusion does not occur prior to severe bilayer leakage.

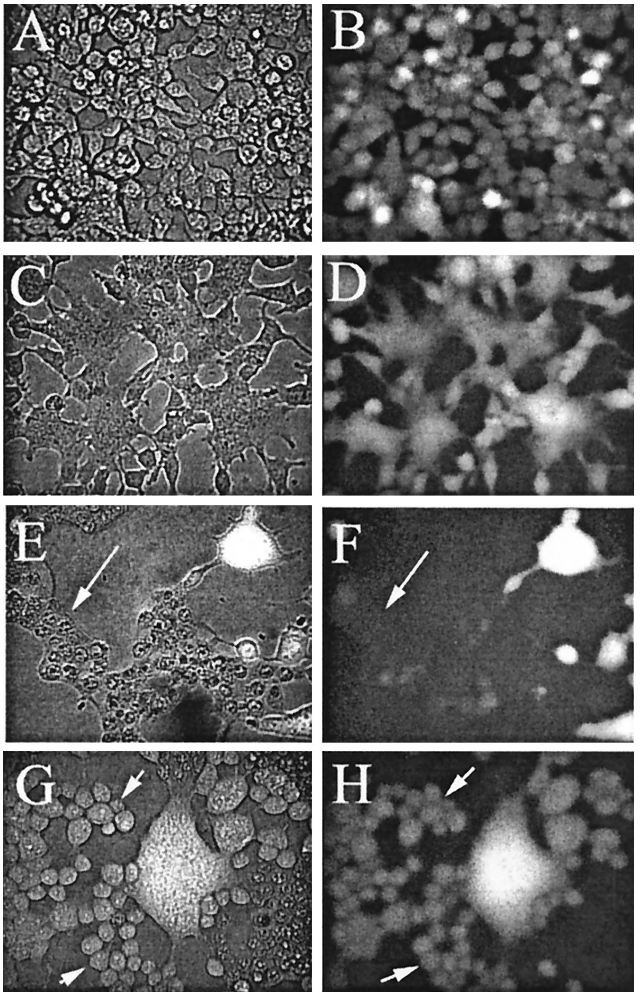

FIG. 3. Cell-cell fusion occurred without loss of aqueous contents for negative potentials but with loss for zero membrane potentials. Calcein-AM was loaded into transfected cells, and cell-cell fusion was induced as described in Materials and Methods. Panels A, C, E, and G are phase-contrast images, and panels B, D, F, and H are fluorescence images. Images in panels A and B were captured prior to lowering of pH. All other images were taken 30 min after the low-pH treatment. Images in panels C and D show cells bathed by a high-Na^+-content medium (i.e., negative potentials). As seen in panel D, calcein was retained by all the fused cells. Images in panels E to H are cells bathed by high-K^+-content medium (i.e., zero voltage). Here, calcein leaked from some of the syncytia (marked by arrows in panels E and F) but not from others (bright syncytia in upper right corner of panel F). All unfused cells (some marked by arrows in panels G and H) retained calcein. Thus, only if cells fused at zero potential did they leak calcein.

curred relatively soon after lowering of pH (within 1 min, typically on the order of 10 s or so). By alternating experiments of *trans*-positive polarity with those of *trans*-negative polarity, we could be certain that any lack of fusion was due to the polarity of voltage and not due to an inability of the cells to fuse. However, because of the limited stability of the bilayer at +40 mV after the lowering of pH, we could not determine whether fusion might have occurred, had the membrane remained stable for longer times. We can be certain, however, that fusion does not proceed without leaks for *trans*-positive potentials. Although fusion did not occur unless both a high concentration of cholesterol and a small amount of a sphingolipid were included in the planar membrane, the leaks did not exhibit this lipid dependence. Leaks occurred for −40 mV after lowering of pH for membranes devoid of cholesterol and sphingolipid. Control experiments with mock-transfected cells did not lead to leaks or other electrical activity, showing that the leaks were induced by E1 and were dependent on low-pH triggering.

We tested whether a *trans*-negative potential was generally required for fusion to occur without leaks by using a target membrane that was quite distinct from a planar bilayer: we measured low-pH-induced syncytium formation between cells expressing the SFV structural proteins. We used ion substitution experiments to change voltage in order to determine whether leakage associated with cell-cell fusion was voltage dependent. Because ion substitution does not conveniently permit positive potentials to be generated inside a cell, we compared fusion of cells at the normal cellular *trans*-negative potential to cells with zero membrane potential. Cells transfected to express E1/E2/E3 were grown to subconfluency and were loaded with the water-soluble dye calcein-AM (Fig. 3A and B). The cells were treated at pH 5.6 for 5 min and returned to neutral pH for 30 min, and syncytium formation was evaluated (Fig. 3C to H). The membrane potential was varied by substituting K^+ for Na^+ in the external solution. Because the membranes of cells at rest are predominantly permeable to K^+, the membrane potential is *trans* negative for high external Na^+ content (Fig. 3C and D) but is close to zero for high external K^+ content (Fig. 3E to H). The extent of syncytium formation for cells with high external Na^+ content was the same as that for high external K^+ content. However, a significant fraction of the syncytia that formed when high K^+ con-

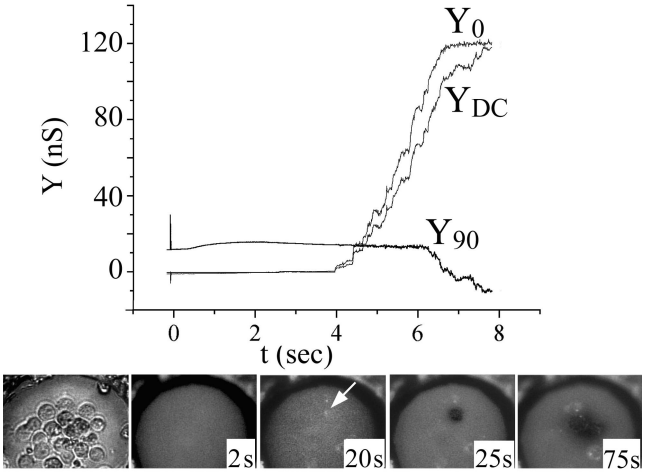

FIG. 4. E1/E2-expressing cells can hemifuse with planar membranes. All conditions were the same as for Fig. 1 with a potential of −40 mV applied to the *trans* solution. As shown in the electrical traces, Y_{90} did not increase after reduction of pH, but both Y_0 and Y_{DC} did increase. The large increases in Y_0 and Y_{DC} eventually corrupted the setting of the phase angle, causing the artifactual decrease in Y_{90} at 6 s. As shown in the lower images, some cells brightened due to the spread of rho-PE, showing that hemifusion occurred (arrow at 20 s). Because Y_0 was somewhat greater than Y_{DC}, small pores or leaks may have developed in the hemifusion diaphragm. Eventually full fusion could occur, seen here by the darkening of the planar membrane (image at 25 s) at the site of the previously hemifused cell. First image, bright-field microscopy; subsequent images, fluorescence.

tent was present became very leaky and lost the calcein marker (Fig. 3F, arrow), whereas all syncytia that formed with high Na^+ content retained the marker (Fig. 3D). If the cells did not fuse, leaks did not occur: for high K^+ content, the cells that did not fuse retained the calcein (Fig. 3G and H, left). Because the cells should be depolarized to about 0 mV by the high external K^+ content, the extent of cell-cell fusion was not strongly voltage dependent. These measurements did not indicate, however, whether the kinetics of fusion were voltage dependent over this range or whether cell-cell fusion would be blocked by a *trans*-positive membrane potential. From these results, however, it is clear that, for cell-cell fusion to be tight and devoid of leaks, a *trans*-negative membrane potential was required.

For some batches of transfected cells fusion to planar bilayers did not occur. But for these batches, hemifusion often did occur between the cells and planar bilayer for voltage equal to −40 mV ($n = 25$). This hemifusion was observed as brightening of the cells, caused by spread of rho-PE (e.g., arrow in Fig. 4, middle image). Electrically, a slow increase in Y_0 that was greater than the increase in Y_{DC} (Fig. 4) typically occurred prior to dye spread. This indicated that an electrical connection between the cell interior and *trans* solution was established through the hemifusion diaphragm (40). (A hemifusion diaphragm separates the interior of the cell from the *trans* solution of the bilayer. It must be a pure lipid bilayer, devoid of protein: if protein were to reside within the diaphragm, the protein ectodomain would have transferred from the extracellular solution to cytosol, which is physically impossible.) The initial increases in Y_0 were not entirely smooth; at certain points they were small and stepwise. This pattern of increases could indicate that small, nonenlarging pores were forming within a hemifusion diaphragm. If they were, it would mean that lipid dye had spread through the hemifusion diaphragm slowly because these small pores would have formed (i.e., at times between 4 and 8 s) prior to a detectable amount of dye spread. In a few cases, after a cell started to become bright due to movement of the rho-PE (i.e., hemifusion occurred), Y_{90} increased in a stepwise fashion (data not shown), and a darkening at the site on the planar membrane below the previously brightened cell (Fig. 4, image at 25 s) was observed ($n = 5$). Thus, a cell that hemifused could still support subsequent pore formation (darkening shown in last two images of Fig. 4). In some cases, a bright spot would remain during cell darkening, indicating that the pore formed outside the previously formed hemifusion diaphragm.

Zn^{2+} and trypan blue inhibit fusion of E1/E2 cells to planar bilayer membranes. In order to verify that E1/E2-induced fusion was the same for planar bilayers as target membrane as it was for liposomes and cells as targets, we tested whether features shown for these other target membranes also held for planar bilayers.

Studies of fusion between SFV and liposomes containing sterols other than cholesterol have shown that a sterol must contain 3β-OH. Fusion did not occur when epicholesterol, identical to cholesterol except that it contains 3α-OH rather than 3β-OH, was included in liposomal membranes (26). Other features of cholesterol, such as planarity of its four-membrane sterol ring or its precise side chain, are of less consequence in fusion (26). In agreement with the importance of 3β-OH, we found that planar bilayer membranes that contained SM and either epicholesterol or cholesterol acetate did not support fusion or hemifusion, as assayed both electrically and by the absence of the spread of rho-PE. However, nonspecific conductance increases did occur upon reduction of pH (data not shown). Thus, it appears that at low pH the envelope proteins interacted with planar membranes containing these cholesterol analogs but that the interactions did not produce fusion.

Wild-type SFV shows very inefficient fusion and infection of cholesterol-depleted cells, while an SFV mutant termed srf-3 shows increases of about 100-fold in infection and 500-fold in fusion, due to a single E1 mutation of proline 226 to serine (60). We compared the fusion properties of wild-type and P226S envelope proteins using the planar bilayer system. In agreement with liposome experiments (4), the wild type and mutant exhibited equivalent fusion for cholesterol-containing membranes and showed comparable kinetics and voltage dependence in the planar bilayer assay. Although the srf-3 mutant is markedly less cholesterol dependent than wild-type virus, it still shows a strong preference for membranes containing cholesterol (4, 60). We did not observe fusion of srf-3-expressing cells with cholesterol-free planar bilayers, presumably reflecting that only a small number of cells are present and thus the system is not suitable for studying low-probability fusion events.

Zn^{2+} inhibits fusion of SFV to liposomes (9) and trypan blue blocks fusion of E1/E2/E3-expressing cells to target cells (30). We found that 1 mM Zn^{2+} eliminated fusion while 100 μM trypan blue partially blocked fusion and 250 μM trypan blue

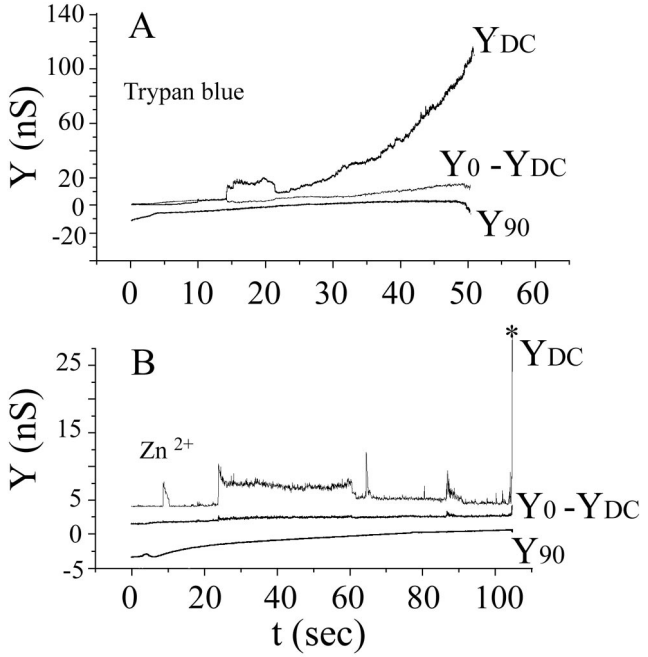

FIG. 5. Trypan blue and Zn^{2+} inhibited fusion but not bilayer conductance increases. All conditions were the same as for Fig. 1 with a potential of −40 mV applied to the *trans* solution. Trypan blue (250 μM) (A) or 1 mM Zn^{2+} (B) was added to the *cis* solution after settling of the cells on the planar membrane and before pH treatment. Fusion did not occur after reduction of pH, as seen by the absence of increases in Y_{90} and the finding that $Y_0 = Y_{DC}$. The conductance of the planar membrane (Y_{DC}) increased in a smooth fashion in the presence of trypan blue and in step-like fashion in the presence of Zn^{2+}. The conductance increases were much greater in the presence of trypan blue than in the presence of Zn^{2+} (note the differences in scales). The membrane ruptured from a small conductance in the presence of Zn^{2+} (marked by the asterisk in panel B) and in the presence of trypan blue (A), after the membrane became very leaky.

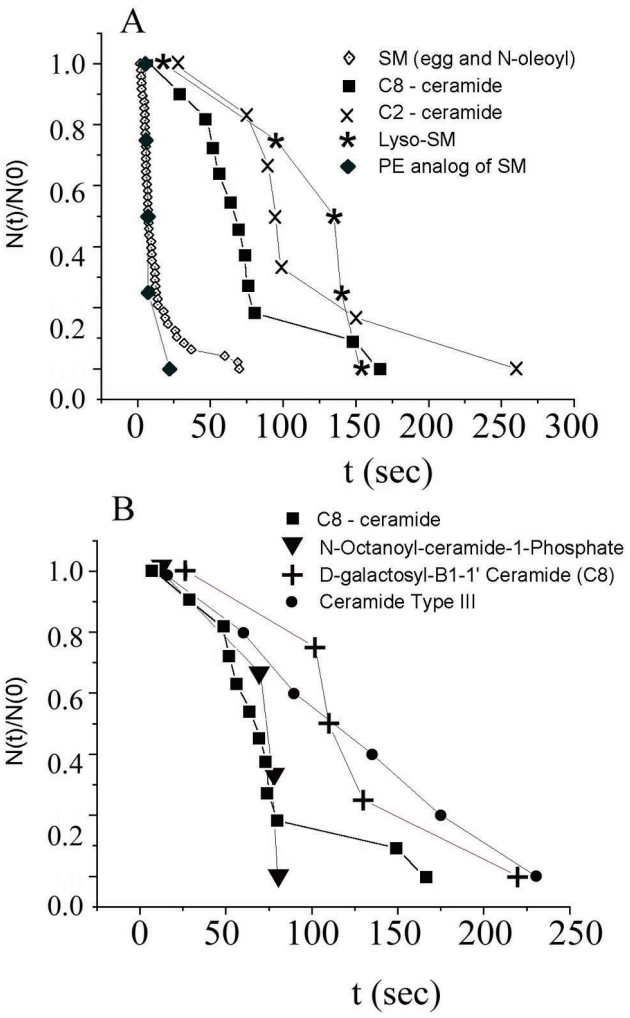

FIG. 6. The dependence of fusion kinetics on sphingolipid structure. Experimental conditions were the same as for Fig. 1 except that SM was replaced with the indicated sphingolipid. Waiting-time distributions were generated (see Materials and Methods). (A) SM and ceramide-PE yielded faster kinetics of fusion than did the ceramides. Lyso-SM supported fusion with kinetics comparable to those of the ceramides. (B) The kinetics of fusion for ceramides or cerobrosides in the planar bilayer membrane were similar. Neither the precise head group of the cerobroside nor the length of the amide-linked acyl chain on the ceramide strongly affected kinetics.

completely blocked fusion (Fig. 5): both inhibitors blocked the increases in Y_{90} that characterize fusion and eliminated lipid dye spread. Interestingly, nonspecific conductance increases (i.e., $Y_{DC} = Y_0$) still occurred when the pH was lowered in the presence of either inhibitor. In the case of Zn^{2+}, fluctuating step-like conductance changes were observed and the conductance increased by only several nanosiemens, before the membrane suddenly ruptured (Fig. 5B), whereas for trypan blue the conductance increases were generally smooth as they rose to large values (i.e., to hundreds of nanosiemens) prior to membrane rupture (Fig. 5A). These leaks are presumably consequences of membrane insertion of E1, which has been shown to occur in the presence of Zn^{2+} (9).

The sphingolipid dependence of SFV E1-induced fusion for planar bilayers. Cholesterol must constitute a high moles percent (on the order of 30%) of a target membrane to optimally support fusion (61). Considerably smaller amounts of sphingolipids (about 2 to 5 mol%) are required with the cholesterol to optimally promote fusion (44). The presence of cholesterol is essential for binding of SFV to liposomes after lowering of pH (26, 44); the same cholesterol-dependent binding occurs for a water-soluble, proteolytically isolated ectodomain of E1 (27). The presence of sphingolipids in liposomes significantly augments low-pH-dependent binding of the soluble ectodomain (27). Both cholesterol and sphingolipids also promote the low-pH-dependent structural changes of E1 (4, 10, 27, 44). Although sphingosine is the backbone of all sphingolipids, sphingosine alone in liposomes does not support fusion (44). The minimal structure that had been found to support fusion was C_8-ceramide, sphingosine with a C_8 acyl chain attached (10).

We used waiting-time measurements to explore the kinetics of fusion with planar bilayers containing various sphingolipids (Fig. 6). In agreement with previous liposome data (10, 44), sphingosine did not support fusion (data not shown). However, adding either an acyl chain (yielding a ceramide) or an appropriate head group to sphingosine yielded a lipid that supported

fusion (Fig. 6A). As previously reported for liposomes (10), incorporation of C_8-ceramide into planar bilayers supported fusion. We found that even a very short acyl chain on sphingosine (C_2-ceramide) supported fusion with kinetics comparable to those of other ceramides (Fig. 6A). Although ceramides supported fusion, they were not as effective as SM, as demonstrated by the significantly longer waiting times: with SM (either egg SM or *N*-oleoyl-SM, each at 5 mol%) in the bilayer, the delay until fusion was only ~3 to 10 s (Fig. 6A). The delay was much longer (~50 to 150 s) for ceramides, even those with long acyl chains (e.g., ceramide type III, which has predominantly saturated acyl chains, mostly 18:0) (Sigma catalog) (Fig. 6B). The faster kinetics of fusion for SM observed here contrast with the results of population studies of SFV-liposome fusion, where the kinetics were similar for SM ceramides (42, 44).

Attachment of the phosphorylcholine head group onto ceramide produces SM; the attachment of phosphorylethanolamine produces the ethanolamine analog ceramide-PE. Ceramide-PE supported fusion with the same rapid kinetics that SM did (Fig. 6A), while other head groups (e.g., ceramide-1-phosphate or galactosyl-ceramide) yielded slower fusion kinetics similar to those observed with ceramides (Fig. 6B). The ganglioside $Gd1_a$ did not support fusion (data not shown), even though it is a sphingolipid. It is possible that the two negative charges of $Gd1_a$ and/or the hydrophilic polar head group (which is massive compared to that of ceramides) inhibit interaction with the SFV fusion protein. Thus, the fact that the head group of SM is larger than that of a ceramide was not the cause of faster fusion: the specific structure of the phosphorylcholine (or phosphorylethanolamine) head group of SM must be involved. This head group effect is underscored by the finding that sphingosylphosphorylcholine (i.e., lyso-SM) also mediated SFV E1-induced fusion of 293T cells with planar membranes (Fig. 6A). In other words, it is not essential that an acyl chain be added to sphingosine to produce fusion—the phosphorylcholine head group could be added instead. However, the mere addition of a head group to sphingosine is not adequate, as demonstrated by the finding that sphingosine-1-phosphate did not support fusion (data not shown). The kinetics of fusion were similar when either lyso-SM or ceramides were included in the planar membrane, and all were appreciably slower than the kinetics observed with SM (Fig. 6). Interestingly, fusion was observed with lyso-SM even though this lipid should have positive spontaneous curvature that should significantly inhibit fusion, when included at 10 mol% in the absence of a compensatory negative spontaneous curvature lipid. We thus conclude that, with planar bilayers as target membranes, any ceramide supports fusion, that either an acyl chain or an appropriate head group can be coupled to sphingosine to induce fusion, and that the polar head group phosphorylcholine (or phosphorylethanolamine) greatly facilitates fusion. (We hypothesize in Discussion and the Fig. 8 legend why fusion is promoted by the addition to sphingosine of either an acyl chain or an appropriate head group, even though they are oriented in the opposite direction with respect to the membrane-solution interface.)

The sphingolipid requirements for SFV-liposome fusion. The results from the cell-planar bilayer fusion system were compared to results obtained from virus-liposome fusion studies. For these experiments, we followed the fusion of purified pyrene-labeled SFV by monitoring the loss of the pyrene excimer peak at 480 nm due to dilution of the pyrene label upon fusion of labeled virus with unlabeled liposomes (2, 4). We used this lipid mixing assay to test the ability of C_2-ceramide to support SFV fusion. The standard convention used in virus-liposome fusion experiments is to refer to the observed lipid mixing as fusion, but one should bear in mind that such lipid mixing could represent either hemifusion or full fusion. Liposomes were prepared based on the lipid composition (i.e., DOPC-DOPE) of the planar bilayers (Fig. 7). In agreement with previous experiments (2, 4), SFV fused very efficiently with control liposomes containing SM and cholesterol (Fig. 7, trace b), with ~70% fusion observed within 10 s after treatment at pH 5.5. Similar to results with the planar bilayers, C_2-ceramide supported fusion almost as efficiently as SM, with ~55% fusion within 10 s (trace c). Little fusion was observed using liposomes containing no sphingolipid (trace e) or liposomes without cholesterol (data not shown). Thus, under these conditions there was good agreement between the fusion activity in the cell-planar bilayer assay and results using virus and liposomes. In separate experiments we found that C_2-ceramide did not support fusion when egg PC and PE replaced DOPC-DOPE but that it was active in this lipid mixture containing a higher molar ratio of cholesterol (data not shown). Thus, the

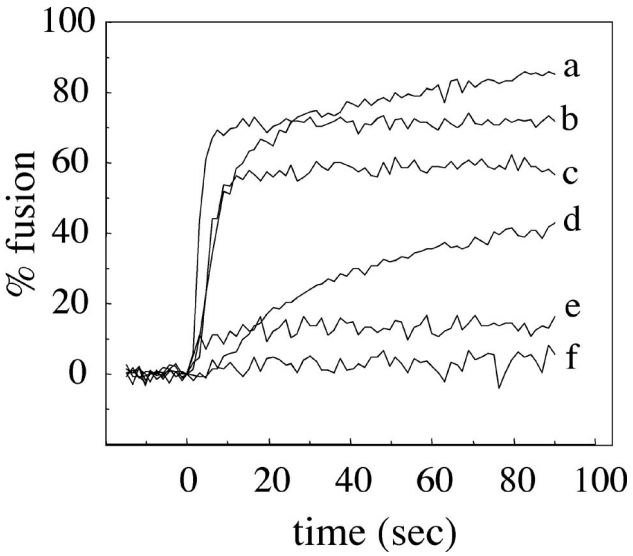

FIG. 7. Fusion of pyrene-labeled SFV with liposomes containing various lipid compositions. Real-time fluorescence recordings of fusion of pyrene-labeled SFV (0.6 μM phospholipid) with the indicated liposomes (200 μM lipid) at 22°C. The liposome compositions were based on DOPC-DOPE-cholesterol (in moles percent, 41/29/22), plus the indicated sphingolipid or ceramide at 8 mol%. The specific sphingolipid component and any added fatty acid are as indicated for each liposome type. Each curve is the average of two independent experiments. Liposomes are sphingolipid deficient with free AA (50 μM) (a) or control, containing SM (b); or contain C_2-ceramide (c); contain lyso-SM plus free AA (50 μM) (d); are sphingolipid deficient (e); or contain lyso-SM (f). For samples b, c, e, and f, liposomes and virus were mixed, the samples were preequilibrated for 3 min at 22°C, and the pH was adjusted to 5.5 at time zero. For samples a and d, liposomes plus AA were preequilibrated for 5 min at 22°C. Pyrene-labeled virus was then added at $t = -15$ s, and the mixture was adjusted to pH 5.5 at time zero.

fusion activity of a particular sphingolipid is influenced by the phospholipid and sterol composition of the target membrane.

We tested whether lyso-SM supported fusion when included in a DOPC-DOPE liposome containing cholesterol. It did not support fusion either under these conditions (Fig. 7, trace f) or in the other liposome compositions described above (data not shown). We reasoned that E1 of SFV might be activated by lyso-SM but that the inverted cone shape of lyso-SM (conferring positive spontaneous curvature to the monolayer into which it is incorporated) inhibited hemifusion, as is known to occur for other viruses and other lysolipids (6). Indeed, exogenously added lyso-SM inhibited SFV fusion with complete liposomes (15 μM lyso-SM blocked fusion by 29 to 71%, depending on the PC and PE composition, data not shown).

To further assess the consequences of lipid shape (5) on lipid mixing, we tested the ability of exogenous arachidonic acid (AA) to promote lipid mixing with liposomes containing lyso-SM. AA is a cone-shaped lipid that complements the inverted cone shape of lyso-SM. It confers negative spontaneous curvature and promotes hemifusion (6). Although AA increased lipid mixing with lyso-SM liposomes (compare traces d and f in Fig. 7), it unexpectedly increased lipid mixing even more dramatically with liposomes that did not contain any sphingolipid (compare traces e and a in Fig. 7). The increased lipid mixing caused by AA was dependent on low-pH treatment (Fig. 7, no lipid mixing observed prior to acid treatment at time zero) and on the presence of cholesterol in the liposome (data not shown). Thus, the lipid mixing induced by AA addition was dependent on the stable insertion of the E1 fusion protein. Taken together, the liposome data show that C_2-ceramide can support fusion but that its activity is influenced by the liposome composition, that AA promotes lipid mixing in the absence of sphingolipids, and that any fusogenic activity of lyso-SM is obliterated by its unfavorable inverted cone shape.

DISCUSSION

Three unanticipated discoveries about E1/E2 fusion emerged from the present study. The first surprising finding was that *trans*-negative potentials kinetically promote virus fusion with planar bilayer membranes. The second was that, for cells to fuse without leakage, either to a planar bilayer or among themselves, a *trans*-negative membrane potential had to be maintained. The third was that the attachment of either a minimal acyl chain or a phosphorylcholine head group to sphingosine produces a sphingolipid that supports fusion.

Membrane potential as a factor in the fusion of SFV. SFV was the first virus shown to require a low pH in order for fusion to occur (19, 61). Increasing the pH of the interiors of endosomes by either directly inhibiting the vacuolar H^+-ATPase with concanamycin A or bafilomycin A_1 (17) or by dissipating the proton gradient with the ionophores nigericin and monensin (37) blocked SFV fusion.

Experiments in which extracellular sodium was replaced by other ions had indicated that low-pH-triggered fusion between virus and endosomes might be dependent on the polarity of the endosomal membrane potential (20). But the evidence was indirect and not fully self consistent and was never followed up. In the present study we have provided direct evidence that the kinetics of SFV E1-induced fusion are accelerated by a *trans*-negative potential when a planar lipid bilayer is the target membrane and that this fusion occurs without leaks. Fusion did not occur for a *trans*-positive potential after lowering of pH at times and under conditions that supported fusion with a *trans*-negative potential. Because of bilayer leaks and rupture, we could not determine whether fusion would have occurred for a *trans*-positive potential at long times after the pH was lowered. But clearly, SFV E1 induced substantial leaks prior to any fusion that could occur for *trans*-positive potentials. As is well known, SFV readily fuses to liposomes without the need to create a *trans*-negative potential. Here some leakage is observed (58), but the temporal order of fusion and leakage has not yet been determined. We have now shown that cell-cell fusion also requires a *trans*-negative membrane potential for nonleaky fusion to occur. Therefore, it appears that, independent of the target membrane, fusion without leaks requires a *trans*-negative potential. The fusion of any virus that requires the low pH within an endosome, including SFV, must occur prior to leakage because, if the endosomal membrane were to develop any leaks, the pH within the endosome would become neutral. It is likely that the generation of the pH gradient across an endosomal membrane leads to a *trans*-negative (i.e., negative compared to that of the endosome interior) potential (14, 18). Our experiments suggest that in the biological situation the generation of a *trans*-negative potential across the endosomal membrane would be essential to promote fusion.

Membrane potential is definitely not a factor in fusion of several other viruses where the studies have allowed rigorous

FIG. 8. Requirements for C-2–C-3 rotation around their bond. (A) The structure of the two stereoisomers of SM, D-*erythro* and L-*threo*, is shown. The positions of hydrogen bond donors and acceptors are indicated by asterisks. The C-2–C-3 axis is indicated by the arrow. The orientation of the hydrogen bond donors and acceptors as well as of the head group of SM viewed along the C-2–C-3 axis is shown in the detached blowup where "a" represents a hydrogen bond acceptor, "d" is a donor, and "a-d" is a hydroxyl that can serve as either an acceptor or donor. Clearly the structures formed by the hydrogen bond donors and acceptors are quite distinct for the two stereoisomers; thus, one (D-*erythro*) form but not the other can, on first principles, specifically interact with SFV E1. Most significantly, the hydroxyl group on C_3 points into the page (i.e., down) for D-*erythro* but out of the page (i.e., up) L-*threo*. (B) The Neuman projection (see www.uic.edu/~kbruzik/text/chaper6.htm for a description of Neuman projections), shown on the left, shows the molecule along the C-2–C-3 axis, with C-2 in front projecting three branches (e.g., to H-21, C-1, and N), and C-3 in the back (beneath C-2 in this view) represented by a circle with its three outgoing bonds (to C-4, OH, and H-31). In the side view of the lipids, the straight arrow (shown for C_2-ceramide) represents the C-2–C-3 axis and the counterclockwise arrow indicates rotation around the C-2–C-3 bond. As illustrated in the top row, the hydrogens of C-2 (H-21) and C-3 (H-31) can assume an antiperiplanar configuration for sphingosine, C_2-ceramide, and lyso-SM. But as illustrated in the bottom row, these hydrogens can exist in a synclinal orientation only for sphingosine. The acyl chain of a ceramide would have to enter the aqueous phase and the polar head group of lyso-SM would have to partition into the hydrocarbon portion of the membrane for the synclinal orientation to occur.

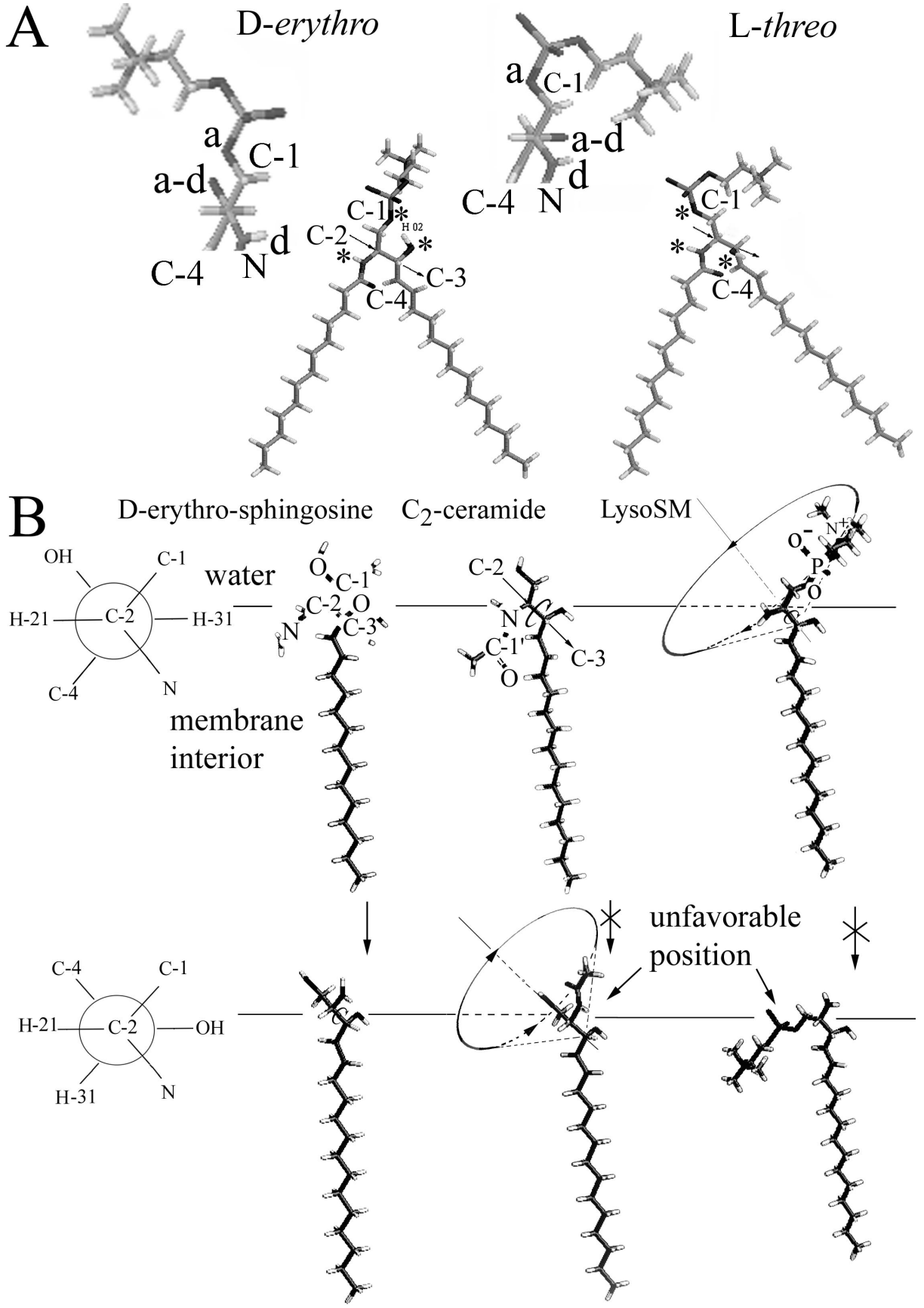
A
D-erythro
L-threo
a
C-1
a-d
d
C-4
N
C-2
C-3
H 02
B
D-erythro-sphingosine
C2-ceramide
LysoSM
OH
H-21
H-31
water
membrane
interior
unfavorable
position

control of the potential. Influenza HA fusion (51), baculovirus gp64 fusion (47), and human immunodeficiency virus type 1 Env-mediated fusion (38) are independent of the potential of the target membrane. Their fusion proteins probably interact with target membranes in a manner independent of voltage. Because the kinetics of fusion and leakage induced by SFV E1 depend on voltage, it appears that the precise interactions of SFV E1 with membranes vary with voltage. The fusion peptides, a stretch of nonpolar amino acids that insert into target membranes, of the viral fusion proteins of influenza virus, baculovirus, and human immunodeficiency virus are at the N terminus of the fusion subunit. In contrast, E1 has an internal fusion peptide, roughly amino acid residues 80 to 96, flanked by charged amino acids (15, 25, 31, 32). It is possible that voltage-dependent interactions occur only in viruses in which the fusion protein contains an internal fusion peptide. The fusion protein of vesicular stomatitis virus also has an internal fusion peptide (63), and ion substitution experiments, similar to those performed for SFV (20), indicate that a *trans*-negative potential promotes fusion (1). For some bacterial toxins, notably colicins, hydrophobic internal segments spontaneously insert as a hairpin into a target membrane at low pH and then a *trans*-negative potential drives other segments of the protein into the membrane (23, 41, 48). Thus, it is possible that this common process used by bacteria to insert toxins into membranes also occurs in a viral system, that of SFV E1 fusion. The finding that hemifusion tended to occur at *trans*-negative potentials for batches of cells that did not fully fuse suggests that the voltage-dependent steps occur upstream of the steps leading to hemifusion. SFV is a member of a class of viruses whose fusion proteins probably do not form six-helix bundles (31). Alternate possibilities for the observed voltage dependence are that a *trans*-negative membrane potential is utilized only by this class of viral proteins or that there is a relationship between the need for *trans*-negative potentials and particular lipids.

Common sense dictates that some portion of E1 must interact with the target membrane before cholesterol, sphingolipids, or membrane potential can further affect the protein. Even when fusion was prevented by either adding Zn^{2+} or trypan blue to the *cis* solution or by not including cholesterol or SM in the planar bilayer, we observed conductance increases. Therefore, the leaks may be a consequence of an initial low-pH-triggered E1-membrane insertion. The fusion peptide or a flanking region is the likeliest candidate for the portion of E1 that initially interacts with the membrane in a reaction that is independent of lipid composition and membrane voltage. Any such E1-membrane interactions are presumably reversible because neither virus nor E1 ectodomains cofloat with cholesterol-free liposomes (26, 27, 44).

A comparison between fusion of E1-expressing cells with planar bilayer membranes and SFV with liposomes. The present planar bilayer studies and results from previously described virus-liposome fusion revealed that these two systems both showed efficient membrane fusion that was dependent on low-pH treatment, cholesterol, and sphingolipid. It is well known that viral fusion can be reliably studied by fusing cells that express the fusion proteins to target cells containing the necessary receptors; thus, the presence of endogenous cellular proteins does not greatly perturb the fusion process. In the case of SFV, the finding that cells expressing E1/E2 support fusion basically identical to that of intact virus indicates even more: the icosahedral structure of SFV confers a symmetrical arrangement to E1/E2 at each of the vertices of the virus (31). Either this symmetry is not critical to fusion or, when expressed in cells, the proteins locally associate into the symmetrical arrangement.

The sphingolipid requirement could be fulfilled by C_2-ceramide in either assay system. However, lyso-SM supported membrane fusion only in the planar bilayer system. In the virus-liposome assay the fusion-inhibiting properties of the inverted cone-shaped lyso-SM dominated and were shown to counteract fusion promotion by AA. We do not know why lyso-SM showed such different effects for the two bilayer systems. Three possible explanations follow: (i) the curvature of the liposomes makes them more susceptible to the inhibitory properties of the inverted cone-shaped lyso-SM; (ii) the membrane potential across liposomes is 0 mV; therefore, fusion is less optimal than it would be if a *trans*-negative potential was present, causing factors that would be minor when fusion is optimal to become prominent; and (iii) the lyso-SM forms micelles, and there will always be some lyso-SM in solution that could transfer to virus to inhibit fusion. Strictly speaking, the spread of pyrene-labeled lipids from virus to liposomes monitors hemifusion rather than fusion. Studies with ectodomains (16, 27) and intact virus (26, 44) show that, at low pH, the E1 protein interacts with liposomes containing cholesterol. AA should promote hemifusion downstream of fusion peptide insertion, and it abolishes the requirement for sphingolipids in at least the first step of lipid mixing, further supporting the expectation that a sphingolipid-dependent step is downstream of fusion peptide insertion. The inhibition of lipid mixing by lyso-SM and its promotion by AA suggest that, as is the case for other viruses such as influenza virus, SFV fusion proceeds through a stalk intermediate that is influenced by membrane curvature (6).

A hypothesis for the interaction of E1 with sphingolipids. SFV infects insect cells, but these cells do not contain appreciable amounts of SM; they contain the ethanolamine analog of SM, ceramide-PE (62). Thus, it is notable that we have found that ceramide-PE supports E1-mediated fusion as effectively as does SM. It is likely that specific interactions to promote fusion occur between the sphingolipids and E1 rather than by preferential complexation of sphingolipids with cholesterol into isolated domains such as rafts: the D-*erythro* form of a sphingolipid supports fusion of SFV, but the L-*threo* form does not (42). The very fact that fusion requires a specific stereoisomer with the same stereospecificity for all sphingolipids provides strong evidence that the sphingolipid promotes fusion by interacting with a protein, namely, E1, rather than with cholesterol. Also, the concentration of SM required for fusion (44) is much lower than that required for raft formation in bilayer membranes, and ceramides support fusion but not raft formation in bilayers (13, 52).

Sphingolipids are functionally different from glycerolipids in that sphingolipids can form hydrogen bonds within an individual lipid because their hydroxyl-hydrogens serve as both acceptors and donors. There are, within the backbone region, multiple groups that serve as hydrogen bond donors and acceptors and that can interact with proteins (represented by asterisks in Fig. 8A). Glycerolipids, in contrast, can only form

hydrogen bonds between lipids, not within an individual lipid, and the groups that can serve as donor are in the head group region (e.g., NH_3 groups of PE). The importance of the ability of groups within the backbone region of sphingolipids to serve as donors in hydrogen bonds has long been recognized (46, 53). We propose that the OH groups of C-1 and C-3 and the amide group of C-2 of the sphingosine head group creates a structure in which each group hydrogen bonds with amino acid residues of E1 as part of the fusion process. This structure is quite distinct for the D-*erythro* and L-*threo* forms of a sphingolipid (as illustrated for SM in Fig. 8A). We further propose that, for this structure and E1 to readily form the complex, the structure must be constrained, not able to freely rotate. Specifically, we hypothesize that the addition of either an acyl chain or an appropriate head group to sphingosine allows the resulting sphingolipid to support fusion because rotation would become inhibited around the C-2–C-3 bond (Fig. 8B). Limited flexibility of the sphingosine chain is also important for fusion.

This hypothesis can account for almost all forms of sphingolipid behavior known for E1/E2-induced fusion, as elucidated below.

(i) Sphingosine does not support fusion (44). This can be explained by the structure, as it is able to freely rotate around the C-2–C-3 bond.

(ii) Attaching a minimal acyl chain to sphingosine to produce a ceramide allows for fusion (Fig. 6). The placement of acetate onto the N-amide (producing C_2-ceramide) could prevent rotation around the C-2–C-3 bond because the CH_3 would be confined to the hydrophobic portion of the bilayer. Longer acyl chains should certainly hinder the rotation.

(iii) Adding a phosphorylcholine head group to sphingosine supports fusion (Fig. 6), but the addition of only the phosphate group does not. Rotation should be hindered for lyso-SM. For rotation to occur, the polar head group would have to enter the low dielectric environment of the bilayer, which is electrostatically unfavorable. In contrast, visual inspection indicates that the phosphate of sphingosine-1-phosphate should not have to enter the low dielectric of the membrane for rotation around C-2–C3.

(iv) The 4,5-*trans* carbon-carbon double bond of the sphingosine backbone is necessary for a ceramide to allow fusion (10). Rigidity is key here. The double bond would be more rigidly oriented than the single bond, for which fusion does not occur. Also, because the substituting groups (here, carbons 3 and 6) are on opposite sides of the carbon bond, a kink is not introduced by the double bond, maintaining rigidity. On the other hand, a *cis* double bond (substitutions on the same side of the double bond) would introduce a kink and thereby increase flexibility.

(v) The 3β-OH group of the sphingosine is required for fusion to occur (10). Removing the OH group from the structure eliminates the ability of the resulting lipid to participate as a donor in a hydrogen bond. Here it is not the rotation per se that is important but rather the inability of the sphingolipid to hydrogen bond to the E1/E2.

(vi) Only the D-*erythro* stereoisomer of the sphingolipid supports fusion; the L-*threo* form does not (42). High-resolution nuclear magnetic resonance spectroscopy shows that rotation around the C-1–C-2 bond is restricted for the naturally occurring D-*erythro*, whereas this rotation is unrestricted for the synthetic L-*threo*-SM (3). Because the two isomers also differ in the fractional populations of rotamer around the C-2–C-3 bond (the D-*erythro* is predominantly antiperiplanar, whereas L-*erythro* is predominantly in the positive synclinal conformation) (3), the two isomers have differently oriented hydrogen bond donors and acceptors. The structure would have to be correctly oriented to bond to E1/E2.

(vii) The structure of the head group attached to a ceramide does not generally strongly affect fusion activity (Fig. 6). The precise head group should not affect the orientation of the hydrogen-bonding groups with respect to each other nor their rotation. The ganglioside $Gd1_a$ did not support fusion, but its huge head group could introduce steric interferences.

The proposal that constrained orientations of a spingolipid favor fusion may also account for our finding that SM (or ceramide-PE) was more effective than ceramides in supporting fusion (Fig. 6) but does not necessarily do so. Intramolecular hydrogen bonds between acceptors and donors of SM may control its head group conformation, as proposed previously (3), and this conformation may be optimal for interacting with E1. But clearly either the phosphorylcholine or phosphorylethanolamine head group, perhaps through a dipole potential, promoted the required interactions with E1. The specific interactions between sphingolipids and E1 may be an important step in the conversion of E1/E2 heterodimers to fusion-active E1 homotrimers.

ACKNOWLEDGMENTS

We thank Sofya Brener for technical assistance and Xinyong Zhang and Anna Ahn for assistance with construction of the pCB3 expression vector.

Support was provided by NIH grants GM27367 (to F.S.C.) and GM57454 (to M.K.).

REFERENCES

1. **Akeson, M., J. Scharff, C. M. Sharp, and D. M. Neville, Jr.** 1992. Evidence that plasma membrane electrical potential is required for vesicular stomatitis virus infection of MDCK cells: a study using fluorescence measurements through polycarbonate supports. J. Membr. Biol. **125:**81–91.
2. **Bron, R., J. M. Wahlberg, H. Garoff, and J. Wilschut.** 1993. Membrane fusion of Semliki Forest virus in a model system: correlation between fusion kinetics and structural changes in the envelope glycoprotein. EMBO J. **12:**693–701.
3. **Bruzik, K. S.** 1988. Conformation of the polar head group of sphingomyelin and its analogues. Biochim. Biophys. Acta **939:**315–326.
4. **Chatterjee, P. K., M. Vashishtha, and M. Kielian.** 2000. Biochemical consequences of a mutation that controls the cholesterol dependence of Semliki Forest virus fusion. J. Virol. **74:**1623–1631.
5. **Chen, Z., and R. P. Rand.** 1997. The influence of cholesterol on phospholipid membrane curvature and bending elasticity. Biophys. J. **73:**267–276.
6. **Chernomordik, L., M. M. Kozlov, and J. Zimmerberg.** 1995. Lipids in biological membrane fusion. J. Membr. Biol. **146:**1–14.
7. **Chizmadzhev, Y. A., P. I. Kuzmin, D. A. Kumenko, J. Zimmerberg, and F. S. Cohen.** 2000. Dynamics of fusion pores connecting membranes of different tensions. Biophys. J. **78:**2241–2256.
8. **Corver, J.** 1998. Membrane fusion activity of Semliki Forest virus. Ph.D. thesis. Gröningen University, Gröningen, The Netherlands.
9. **Corver, J., R. Bron, H. Snippe, C. Kraaijeveld, and J. Wilschut.** 1997. Membrane fusion activity of Semliki Forest virus in a liposomal model system: specific inhibition by Zn^{2+} ions. Virology **238:**14–21.
10. **Corver, J., L. Moesby, R. K. Erukulla, K. C. Reddy, R. Bittman, and J. Wilschut.** 1995. Sphingolipid-dependent fusion of Semliki Forest virus with cholesterol-containing liposomes requires both the 3-hydroxyl group and the double bond of the sphingolipid backbone. J. Virol. **69:**3220–3223.
11. **Corver, J., A. Ortiz, S. L. Allison, J. Schalich, F. X. Heinz, and J. Wilschut.** 2000. Membrane fusion activity of tick-borne encephalitis virus and recombinant subviral particles in a liposomal model system. Virology **269:**37–46.
12. **DeTulleo, L., and T. Kirchhausen.** 1998. The clathrin endocytic pathway in viral infection. EMBO J. **17:**4585–4593.
13. **Dietrich, C., L. A. Bagatolli, Z. N. Volovyk, N. L. Thompson, M. Levi, K.**

Jacobson, and E. Gratton. 2001. Lipid rafts reconstituted in model membranes. Biophys. J. **80:**1417–1428.
14. **Fuchs, R., P. Male, and I. Mellman.** 1989. Acidification and ion permeabilities of highly purified rat liver endosomes. J. Biol. Chem. **264:**2212–2220.
15. **Garoff, H., A. M. Frischauf, K. Simons, H. Lehrach, and H. Delius.** 1980. Nucleotide sequence of cDNA coding for Semliki Forest virus membrane glycoproteins. Nature **288:**236–241.
16. **Gibbons, D. L., and M. Kielian.** 2002. Molecular dissection of the Semliki Forest virus homotrimer reveals two functionally distinct regions of the fusion protein. J. Virol. **76:**1194–1205.
17. **Glomb-Reinmund, S., and M. Kielian.** 1998. The role of low pH and disulfide shuffling in the entry and fusion of Semliki Forest virus and Sindbis virus. Virology **248:**372–381.
18. **Hammond, T. G., F. O. Goda, G. L. Navar, W. C. Campbell, R. R. Majewski, D. L. Galvan, F. Pontillon, J. H. Kaysen, T. J. Goodwin, S. W. Paddock, and P. J. Verroust.** 1998. Membrane potential mediates H^+-ATPase dependence of "degradative pathway" endosomal fusion. J. Membr. Biol. **162:**157–167.
19. **Helenius, A., J. Kartenbeck, K. Simons, and E. Fries.** 1980. On the entry of Semliki forest virus into BHK-21 cells. J. Cell Biol. **84:**404–420.
20. **Helenius, A., M. Kielian, J. Wellsteed, I. Mellman, and G. Rudnick.** 1985. Effects of monovalent cations on Semliki Forest virus entry into BHK-21 cells. J. Biol. Chem. **260:**5691–5697.
21. **Hernandez, L. D., L. R. Hoffman, T. G. Wolfsberg, and J. M. White.** 1996. Virus-cell and cell-cell fusion. Annu. Rev. Cell Dev. Biol. **12:**627–661.
22. **Ikonen, E.** 2001. Roles of lipid rafts in membrane transport. Curr. Opin. Cell Biol. **13:**470–477.
23. **Jakes, K. S., P. K. Kienker, and A. Finkelstein.** 1999. Channel-forming colicins: translocation (and other deviant behaviour) associated with colicin Ia channel gating. Q. Rev. Biophys. **32:**189–205.
24. **Kempf, C., U. Kohler, M. R. Michel, and H. Koblet.** 1987. Semliki Forest virus-induced polykaryocyte formation is an ATP-dependent event. Arch. Virol. **95:**111–122.
25. **Kielian, M.** 1995. Membrane fusion and the alphavirus life cycle. Adv. Virus Res. **45:**113–151.
26. **Kielian, M. C., and A. Helenius.** 1984. Role of cholesterol in fusion of Semliki Forest virus with membranes. J. Virol. **52:**281–283.
27. **Klimjack, M. R., S. Jeffrey, and M. Kielian.** 1994. Membrane and protein interactions of a soluble form of the Semliki Forest virus fusion protein. J. Virol. **68:**6940–6946.
28. **Kondor-Koch, C., B. Burke, and H. Garoff.** 1983. Expression of Semliki Forest virus proteins from cloned complementary DNA. I. The fusion activity of the spike glycoprotein. J. Cell Biol. **97:**644–651.
29. **Kurzchalia, T. V., and R. G. Parton.** 1999. Membrane microdomains and caveolae. Curr. Opin. Cell Biol. **11:**424–431.
30. **Lanzrein, M., N. Kasermann, and C. Kempf.** 1992. Changes in membrane permeability during Semliki Forest virus induced cell fusion. Biosci. Rep. **12:**221–236.
31. **Lescar, J., A. Roussel, M. W. Wien, J. Navaza, S. D. Fuller, G. Wengler, and F. A. Rey.** 2001. The Fusion glycoprotein shell of Semliki Forest virus: an icosahedral assembly primed for fusogenic activation at endosomal pH. Cell **105:**137–148.
32. **Levy-Mintz, P., and M. Kielian.** 1991. Mutagenesis of the putative fusion domain of the Semliki Forest virus spike protein. J. Virol. **65:**4292–4300.
33. **Liljestrom, P., and H. Garoff.** 1991. Internally located cleavable signal sequences direct the formation of Semliki Forest virus membrane proteins from a polyprotein precursor. J. Virol. **65:**147–154.
34. **Lu, Y. E., C. H. Eng, S. G. Shome, and M. Kielian.** 2001. In vivo generation and characterization of a soluble form of the Semliki Forest virus fusion protein. J. Virol. **75:**8329–8339.
35. **Mann, E., J. Edwards, and D. T. Brown.** 1983. Polycaryocyte formation mediated by Sindbis virus glycoproteins. J. Virol. **45:**1083–1089.
36. **Marsh, M., and A. Helenius.** 1980. Adsorptive endocytosis of Semliki Forest virus. J. Mol. Biol. **142:**439–454.
37. **Marsh, M., J. Wellsteed, H. Kern, E. Harms, and A. Helenius.** 1982. Monensin inhibits Semliki Forest virus penetration into culture cells. Proc. Natl. Acad. Sci. USA **79:**5297–5301.
38. **Melikyan, G. B., R. M. Markosyan, H. Hemmati, M. K. Delmedico, D. M. Lambert, and F. S. Cohen.** 2000. Evidence that the transition of HIV-1 gp41 into a six-helix bundle, not the bundle configuration, induces membrane fusion. J. Cell Biol. **151:**413–423.
39. **Melikyan, G. B., W. D. Niles, V. A. Ratinov, M. Karhanek, J. Zimmerberg, and F. S. Cohen.** 1995. Comparison of transient and successful fusion pores connecting influenza hemagglutinin expressing cells to planar membranes. J. Gen. Physiol. **106:**803–819.
40. **Melikyan, G. B., J. M. White, and F. S. Cohen.** 1995. GPI-anchored influenza hemagglutinin induces hemifusion to both red blood cell and planar bilayer membranes. J. Cell Biol. **131:**679–691.
41. **Merrill, A. R., and W. A. Cramer.** 1990. Identification of a voltage-responsive segment of the potential-gated colicin E1 ion channel. Biochemistry **29:**8529–8534.
42. **Moesby, L., J. Corver, R. K. Erukulla, R. Bittman, and J. Wilschut.** 1995. Sphingolipids activate membrane fusion of Semliki Forest virus in a stereospecific manner. Biochemistry **34:**10319–10324.
43. **Mothes, W., A. L. Boerger, S. Narayan, J. M. Cunningham, and J. A. Young.** 2000. Retroviral entry mediated by receptor priming and low pH triggering of an envelope glycoprotein. Cell **103:**679–689.
44. **Nieva, J. L., R. Bron, J. Corver, and J. Wilschut.** 1994. Membrane fusion of Semliki Forest virus requires sphingolipids in the target membrane. EMBO J. **13:**2797–2804.
45. **Omar, A., and H. Koblet.** 1988. Semliki Forest virus particles containing only the E1 envelope glycoprotein are infectious and can induce cell-cell fusion. Virology **166:**17–23.
46. **Pascher, I.** 1976. Molecular arrangements in sphingolipids. Conformation and hydrogen bonding of ceramide and their implication on membrane stability and permeability. Biochim. Biophys. Acta **455:**433–451.
47. **Plonsky, I., and J. Zimmerberg.** 1996. The initial fusion pore induced by baculovirus GP64 is large and forms quickly. J. Cell Biol. **135:**1831–1839.
48. **Qiu, X. Q., K. S. Jakes, P. K. Kienker, A. Finkelstein, and S. L. Slatin.** 1996. Major transmembrane movement associated with colicin Ia channel gating. J. Gen. Physiol. **107:**313–328.
49. **Ratinov, V., I. Plonsky, and J. Zimmerberg.** 1998. Fusion pore conductance: experimental approaches and theoretical algorithms. Biophys. J. **74:**2374–2387.
50. **Razinkov, V. I., and F. S. Cohen.** 2000. Sterols and sphingolipids strongly affect the growth of fusion pores induced by the hemagglutinin of influenza virus. Biochemistry **39:**13462–13468.
51. **Razinkov, V. I., G. B. Melikyan, R. M. Epand, R. F. Epand, and F. S. Cohen.** 1998. Effects of spontaneous bilayer curvature on influenza virus-mediated fusion pores. J. Gen. Physiol. **112:**409–422.
52. **Samsonov, A. V., I. Mihalyov, and F. S. Cohen.** 2001. Characterization of cholesterol-sphingomyelin domains and their dynamics in bilayer membranes. Biophys. J. **81:**1486–1500.
53. **Schmidt, C. F., Y. Barenholz, and T. E. Thompson.** 1977. A nuclear magnetic resonance study of sphingomyelin in bilayer systems. Biochemistry **16:**2649–2656.
54. **Simons, K., and E. Ikonen.** 1997. Functional rafts in cell membranes. Nature **387:**569–572.
55. **Simons, K., and G. van Meer.** 1988. Lipid sorting in epithelial cells. Biochemistry **27:**6197–6202.
56. **Siskind, L. J., and M. Colombini.** 2000. The lipids C_2- and C_{16}-ceramide form large stable channels. Implications for apoptosis. J. Biol. Chem. **275:**38640–38644.
57. **Smit, J. M., R. Bittman, and J. Wilschut.** 1999. Low-pH-dependent fusion of Sindbis virus with receptor-free cholesterol- and sphingolipid-containing liposomes. J. Virol. **73:**8476–8484.
58. **Smit, J. M., G. Li, P. Schoen, J. Corver, R. Bittman, K. Lin, and J. Wilschut.** 2002. Fusion of alphavirus with liposomes is a non-leaky process. FEBS Lett. **521:**62–66.
59. **Strauss, J. H., and E. G. Strauss.** 1994. The alphaviruses: gene expression, replication, and evolution. Microbiol. Rev. **58:**491–562.
60. **Vashishtha, M., T. Phalen, M. T. Marquardt, J. S. Ryu, A. C. Ng, and M. Kielian.** 1998. A single point mutation controls the cholesterol dependence of Semliki Forest virus entry and exit. J. Cell Biol. **140:**91–99.
61. **White, J., and A. Helenius.** 1980. pH-dependent fusion between the Semliki Forest virus membrane and liposomes. Proc. Natl. Acad. Sci. USA **77:**3273–3277.
62. **Wiegandt, H.** 1992. Insect glycolipids. Biochim. Biophys. Acta **1123:**117–126.
63. **Zhang, L., and H. P. Ghosh.** 1994. Characterization of the putative fusogenic domain in vesicular stomatitis virus glycoprotein G. J. Virol. **68:**2186–2193.